Proc. Natl. Acad. Sci. USA
Vol. 91, pp. 11631–11635, November 1994
Biophysics

Molecular dynamics simulation of the gramicidin channel in a phospholipid bilayer

T. B. WOOLF AND B. ROUX*

Membrane Transport Research Group (GRTM), Department of Chemistry, Université de Montréal, Montréal, PQ Canada H3C 3J7

Communicated by Martin Karplus, June 27, 1994

ABSTRACT **A molecular dynamics simulation of the gramicidin A channel in an explicit dimyristoyl phosphatidylcholine bilayer was generated to study the details of lipid–protein interactions at the microscopic level. Solid-state NMR properties of the channel averaged over the 500-psec trajectory are in excellent agreement with available experimental data. In contrast with the assumptions of macroscopic models, the membrane/solution interface region is found to be at least 12 Å thick. The tryptophan side chains, located within the interface, are found to form hydrogen bonds with the ester carbonyl groups of the lipids and with water, suggesting their important contribution to the stability of membrane proteins. Individual lipid–protein interactions are seen to vary from near 0 to −50 kcal/mol. The most strongly interacting conformations are short-lived and have a nearly equal contribution from both van der Waals and electrostatic energies. This approach for performing molecular dynamics simulations of membrane proteins in explicit phospholipid bilayers should help in studying the structure, dynamics, and energetics of lipid–protein interactions.**

The scarcity of information about the structure of membrane proteins, along with the complexity of the bilayer environment, makes an understanding of lipid–protein microscopic interactions difficult. Structure prediction algorithms of membrane proteins often represent the membrane/solution interface as a sharp demarcation between a hydrophobic and a hydrophilic environment (1, 2). Such a simplified view may not be sufficient. For example, although the amino acids of membrane proteins are generally distributed according to their hydrophobicity (2), the reasons why tryptophan and other aromatic residues are often found at the membrane/solution interface are not well understood (3). Despite numerous experimental studies, little or no detailed information is available about the microscopic nature of the lipid bilayer/protein bulk solution interface and its implications for lipid–protein interactions. In principle, the powerful molecular dynamics approach for studying biological macromolecules (4) can be used to gain insight into the structure and dynamics of membrane–protein complexes. In practice, extension of current computational methods to simulate a protein in an explicit phospholipid bilayer represents a major challenge. The dynamical stability and the computed properties of the system will depend on two important factors: (*i*) the choice of a carefully constructed starting configuration (5) and (*ii*) the ability of the empirical potential function to represent accurately the balance between hydrophobic and hydrophilic forces. The selection of a model system is important in that a large body of experimental data should be available for assessing the simulation's validity. This paper describes a systematic approach for constructing the starting configuration for molecular dynamics simulations of intrinsic membrane proteins and reports on the results of a 500-psec trajectory for an 8:1 dimyristoyl phosphatidylcholine (DMPC)/gramicidin A (GA) system with 45% (wt/wt) water. All atoms, including the nonpolar hydrogens, were explicitly included in the calculations. The system is a model for the experimental samples investigated by solid-state NMR in the laboratories of Cross (6), Cornell (7), and Davis (8).

The extensively studied transmembrane ion channel formed by GA in a lipid bilayer provides an ideal prototypical model for theoretical investigations of the microscopic details of lipid–protein interactions (9, 10). The three-dimensional structure of the membrane-bound ion-conducting channel is well established: it is an N- to N-terminal dimer formed by two single-stranded right-handed β-helices (6). The pore is lined by the backbone carbonyls, and the side chains—most of them hydrophobic—extend outward into the lipid alkane chains. Four tryptophan residues are located at the end of each monomer near the membrane/solution interface, a structural feature similar to that observed in much larger membrane proteins—e.g., the photosynthetic reaction center (11), annexins (12), and porins (13, 14). The influence of the tryptophans on the lifetime and conductance of the GA dimer channel has been demonstrated (15). Thus, an understanding of the structure and dynamics of the DMPC/GA complex may provide information of fundamental interest about the interactions between the side chains of an intrinsic membrane protein and the surrounding lipids.

A protocol was designed to construct a set of possible starting configurations for the membrane system. Structural data from crystals of phospholipids (16) do not provide an appropriate initial conformation for the lipids in a liquid crystalline bilayer, because extremely long equilibration times would be needed to melt the all-trans frozen alkane chains (5). Moreover, the crystal structures correspond to very low hydration levels, while it is known that ≈20 water molecules are strongly bound to the polar headgroups of phospholipids in a bilayer (17). To construct the possible starting configurations, preequilibrated and prehydrated DMPC molecules were chosen randomly from a set of 2000 (18). One hundred starting configurations were generated and 25 were selected for energy minimization and preparation for dynamics. From this set, 5 systems were chosen for equilibration and trajectory calculations. The results from one trajectory are analyzed in this paper. Further details will be found in a future publication.

THEORY AND METHODS

Microscopic System and Computational Details. The simulation system comprises one GA channel, 16 DMPC molecules, and 649 water molecules. This system is meant to model the oriented samples studied by solid-state NMR (6–8). The experimental samples are prepared with an 8:1

The publication costs of this article were defrayed in part by page charge payment. This article must therefore be hereby marked "*advertisement*" in accordance with 18 U.S.C. §1734 solely to indicate this fact.

Abbreviations: DMPC, dimyristoyl phosphatidylcholine; GA, gramicidin A; vdW, van der Waals.

DMPC/GA molar ratio and 45% (wt/wt) water—i.e., 649 water molecules for 1 GA dimer channel and 16 DMPC molecules. All atoms are represented in the atomic model for a total of 4390 atoms. The potential energy function is the all-hydrogen CHARMM 22 force field (A. D. Mackerell and M. Karplus, personal communication) including the TIP3P water potential (4). In the simulation system, the center of the bilayer membrane is located at $z = 0$ and the channel axis is oriented along the z direction. Hexagonal images in the x–y plane of the bilayer and periodic images normal to the bilayer along the z direction were used to model an infinite multilayer system. The dimensions of the elementary simulation cell are 60 Å along z and 17.2 Å for the edge of the hexagon in the x–y plane. The area of the x–y hexagonal simulation cell is 760 Å^2, which corresponds to the total cross section of 1 GA (250 Å^2) and 8 DMPCs (64 Å^2). The trajectory was calculated in the microcanonical ensemble with constant energy and volume. The average temperature was 340 K, in accord with the experimental conditions (6–8). All bonds involving hydrogen atoms were kept fixed with the SHAKE algorithm (4). The time step was 2 fsec. The system was equilibrated for 100 psec, followed by 500 psec of molecular dynamics. Nonbonded interactions were truncated smoothly at 12 Å for all atom pairs. The calculation required 3 hr of central processing unit (CPU) time per psec (SGI Indigo R4000 computer).

Construction of the Initial Configuration. A special protocol was used to generate a set of 300 initial configurations for the DMPC/GA system. Each configuration was constructed using 16 preequilibrated and prehydrated DMPC molecules (19), chosen randomly from a library of 2000 phospholipid conformers representative of the lipid molecules found in a bilayer membrane in thermal equilibrium (18). The configurations were assembled as a set of rigid units, with each GA or DMPC (with their primary waters) being translated and rotated in a systematic search for an optimum packing. This operation was necessary because a large number of unfavorable core–core overlaps—i.e., atoms that are too close to one another—are present in the random initial configurations. Finally, each configuration was fully solvated and further refined by energy minimization. The resulting model-built membrane–protein complex corresponds to an optimal packing configuration of the phospholipid molecules around the channel and incorporates correctly the experimental data about both chain order and bilayer thickness for a pure bilayer (18, 20). This protocol is a generalization of the approach used by Pastor *et al.* (21) to construct a model of the dipalmitoyl phosphatidylcholine bilayer.

Calculation of NMR Properties. Solid-state NMR properties were calculated to characterize the conformation of the backbone and the side chains of the channel (6–8). To calculate the chemical shift parallel to the magnetic field, $\sigma_\parallel$, a time average of the instantaneous chemical shift tensor projected in the direction normal to the membrane (here the z axis) is used,

$$\sigma_\parallel = \left\langle \hat{\mathbf{Z}} \cdot \left[\sum_{i=1}^{3} \hat{\mathbf{e}}_i(t)\sigma_{ii}\hat{\mathbf{e}}_i(t) \right] \cdot \hat{\mathbf{Z}} \right\rangle, \quad [1]$$

where $\hat{\mathbf{e}}_i(t)$ are the instantaneous unit vectors associated with the ith principal axis and tensor element magnitude σ_{ii} of the static chemical shift tensor for ^{15}N, respectively (6). Similarly, the chemical shift perpendicular to the magnetic field, $\sigma_\perp$ is calculated from an analogous projection of the instantaneous tensor (here in the x–y plane),

$$\sigma_\perp = \frac{1}{2}\left\langle \hat{\mathbf{X}} \cdot \left[\sum_{i=1}^{3} \hat{\mathbf{e}}_i(t)\sigma_{ii}\hat{\mathbf{e}}_i(t) \right] \cdot \hat{\mathbf{X}} + \hat{\mathbf{Y}} \cdot \left[\sum_{i=1}^{3} \hat{\mathbf{e}}_i(t)\sigma_{ii}\hat{\mathbf{e}}_i(t) \right] \cdot \hat{\mathbf{Y}} \right\rangle. \quad [2]$$

The chemical shift anisotropy is defined as $\sigma_\parallel - \sigma_\perp$. The ^{15}N–^{1}H dipolar coupling and the carbon-bonded ^{2}H quadrupolar splittings are both calculated from a time average of the form

$$\langle \Delta\nu \rangle = \Delta\nu_0 \times \left\langle \frac{3\cos^2\theta(t) - 1}{2} \right\rangle, \quad [3]$$

where $\theta(t)$ is the instantaneous angle between the two atoms and the z direction, and $\Delta\nu_0$ is the standard frequency splitting for ^{2}H quadrupolar and dipolar coupling interactions.

RESULTS

Average Structure and Density Profile. The membrane–protein bilayer complex remained stable throughout the 500-psec simulation. Fig. 1 shows one conformation of the simulation system. The transition from the hydrophobic to the hydrophilic environment extends from 9 to 21 Å, with a thickness of about 12 Å. The composition of the interfacial region corresponds to a mixture of water, glycerol, and phosphocholine headgroups. For a pure DMPC bilayer, the thickness of the hydrophobic region has been reported to be 23 Å (20). This corresponds to the region of the DMPC alkane chains. A local minimum in the density of alkane chains is present at the center of the bilayer, as observed both in neutron scattering experiments and in a previous simulation of a dilauroyl phosphatidylethanolamine bilayer (22, 23). The P and N atoms of the polar headgroup are both centered at 16–18 Å, although the N is a little more spread out. The

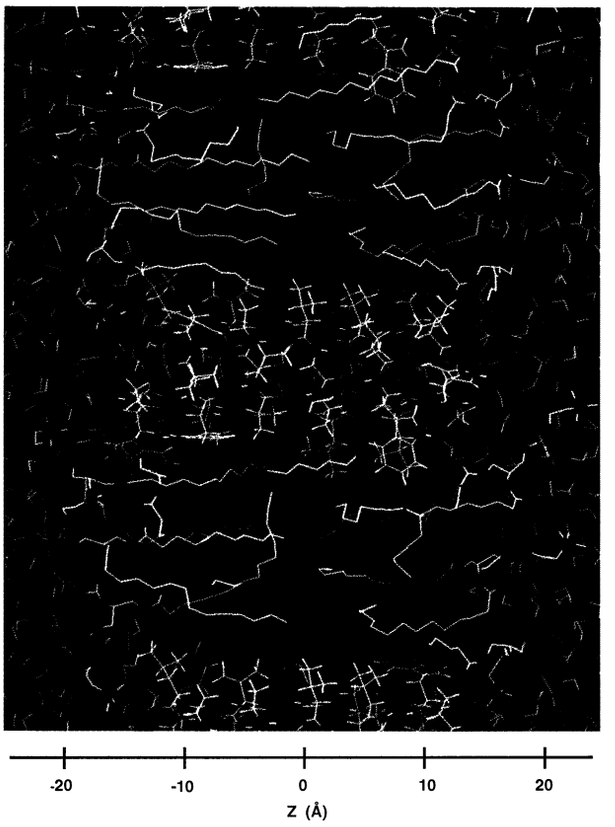

FIG. 1. Structure of the hydrated bilayer/channel system. Representation of the 8:1 DMPC/GA model with 45% (wt/wt) water. Hydrogens of the lipids are not shown, although the model includes all atoms. The nearest image molecules are included in the snapshot. The center of the bilayer is at $z = 0$.

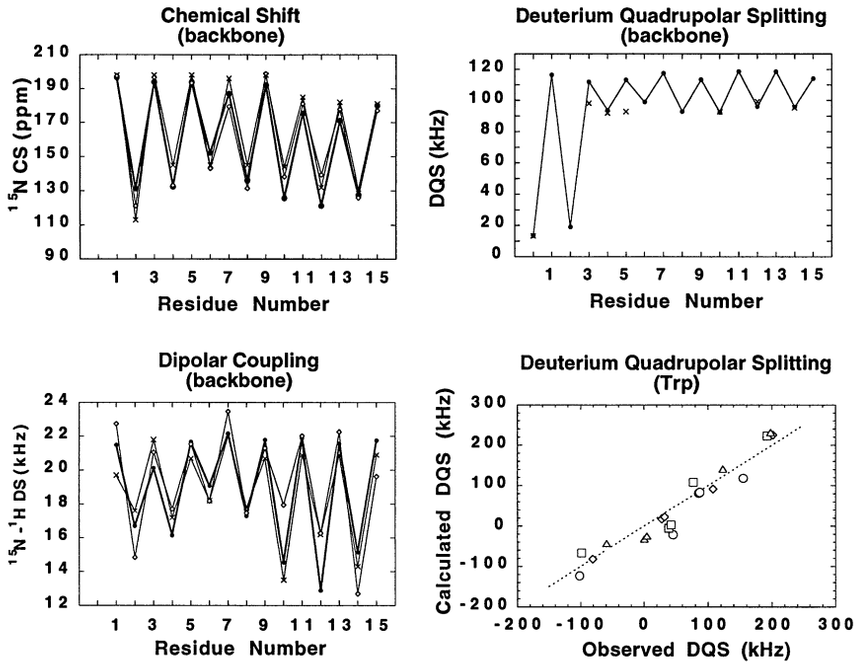

FIG. 2. Solid-state NMR data (x), calculated values from molecular dynamics (●), and values from the static Arseniev structure (◇) obtained by using Eqs. **1–3.** (*Upper Left*) Chemical shift (CS) for ^{15}N sites along the backbone. (*Lower Left*) Dipolar coupling for ^{15}N–^{1}H sites along the backbone. (*Upper Right*) ^{2}H quadrupolar splitting for C$^{\alpha}$ sites along the backbone. (*Lower Right*) ^{2}H quadrupolar splitting (DQS) for the indole ring of tryptophans (○, 9; □, 11; ◇, 13; △, 15).

distribution of the P and N atoms reflects the fact that the P–N vector tends to be almost parallel to the membrane/solution interface. The ester carbonyl groups are located at 12–14 Å.

Comparison with Solid-State NMR Data. To validate the results from a molecular dynamics trajectory, comparison with experimental information is essential. Due to their close relationship with the molecular structure, experimental measurements from solid-state NMR are particularly valuable (6–8). Solid-state NMR data and the calculated values from molecular dynamics are shown in Fig. 2 for the ^{15}N chemical shifts at labeled sites along the backbone (6) (*Upper Left*), the ^{15}N–^{1}H dipolar coupling (6) (*Lower Left*), and the ^{2}H quadrupolar splitting at the C$^{\alpha}$ carbons along the backbone (8) (*Upper Right*). Fig. 2 (*Lower Right*) shows a comparison of the ^{2}H quadrupolar splittings for labeled indole rings (6). The clear alternating pattern of the solid-state NMR backbone properties is evidence for the right-handed helical sense of the GA channel (6). Table 1 shows the ^{15}N chemical shifts and the ^{15}N–^{1}H dipolar couplings for the tryptophans, with values from the Arseniev structure in parentheses (24). The overall agreement between molecular dynamics and solid-state NMR experiment is excellent for both the backbone sites and the tryptophan rings.

The agreement of the static Arseniev structure with solid-state NMR data can be misleading. The slow time-scale of solid-state NMR corresponds to an average over rapidly fluctuating quantities. Based on the calculations, these fluctuations can be large. As an illustration, the distribution functions for three ^{2}H quadrupolar splittings and for the chemical shift of the ^{15}N of Trp^{11} are shown in Fig. 3. The ^{2}H quadrupolar splitting of Hζ3 varies from 0 to 275 kHz; there is an overlap between the Hη2 and Hζ2 splittings, with contributions to the average calculated for the Hη2 spreading from −150 to 75 kHz and from −150 to 200 kHz for the Hζ2 location. Integrating the NMR properties over the distributions of Fig. 3 yields the time averages given in Table 1. Such average distribution functions correspond closely to the spectra that would be observed if the solid-state NMR time scale was made faster than the molecular motions—e.g., as in experiments with fast-frozen low-temperature samples. The broad distributions indicate that large differences can occur between NMR properties averaged over an ensemble of conformations and NMR properties analyzed in terms of a single average structure. Molecular dynamics can provide valuable information for examining relationships between average NMR properties and conformations.

Backbone and Side-Chain Motions. Overall, the membrane does not change the protein conformation significantly: the average rms deviation of GA throughout the trajectory from the initial Arseniev structure is 1.2 Å and fluctuations in the backbone dihedral angles are 11 and 13 degrees for ϕ and ψ, respectively. However, the aliphatic side chains are not restricted by the membrane environment and can make transitions between multiple conformations. During the 500-psec trajectory, transitions between discrete conformational states of the χ_1 and χ_2 dihedral angles were observed for several of the aliphatic side chains. Various types of motion were present—e.g., the χ_1 dihedral transition of Ala^{3} involves the simple rotation of a methyl group. The χ_1 dihedral transitions observed in Val^{1}, Val^{6}, Val^{8}, Leu^{4}, and Leu^{12} and the χ^2 transitions observed for Leu^{4} and Leu^{12} involve more complex atomic motions. Despite the limited experimental

Table 1. Dihedral angles, ^{15}N chemical shifts, and ^{15}N–^{1}H dipolar couplings for the tryptophan residues

	Dihedral angle,* degrees		^{15}N chemical shift,† ppm		^{15}N–^{1}H dipolar coupling,‡ kHz	
Residue	χ_1	χ_2	Calculated	Observed	Calculated	Observed
Trp^{9}	193, 189 (167)	79, 65 (89)	131, 142 (158)	145	17, 19 (13)	13
Trp^{11}	294, 295 (295)	310, 310 (307)	146, 139 (154)	144	10, 9 (11)	11
Trp^{13}	291, 290 (293)	300, 307 (270)	151, 147 (145)	144	15, 12 (9)	10
Trp^{15}	291, 294 (291)	309, 305 (309)	142, 150 (139)	139	8, 10 (6)	8

Numbers in parentheses refer to values calculated from the Arseniev structure (24).
*rms fluctuations in χ_1 and χ_2 were 10 and 15 degrees.
†Tensor component magnitudes were 166, 114, and 36 ppm (6); rms fluctuation in ^{15}N shift was 22 ppm.
‡Dipolar coupling constant $\Delta\nu_o$ = 16 kHz; rms fluctuation in ^{15}N–^{1}H coupling was 10 kHz.

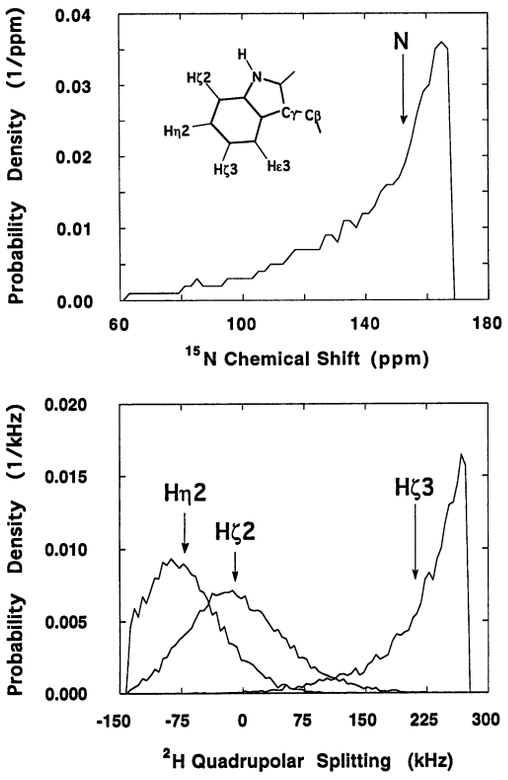

FIG. 3. Average distribution of NMR properties for one monomer of Trp[11]. (*Upper*) Probability density for the chemical shift of ^{15}N on the indole ring. Arrows indicate the average obtained from the trajectory given in Table 1. (*Lower*) Probability density for particular ^{2}H quadrupolar splittings of three sites.

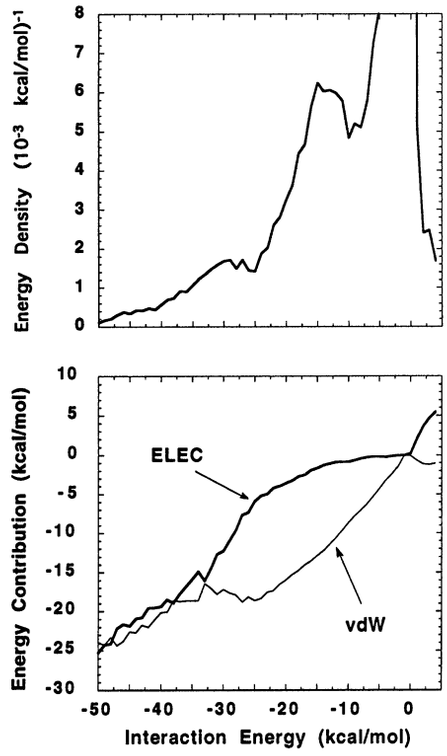

FIG. 4. Average distribution of interaction energies between the GA channel and individual lipids. (*Upper*) Normalized average energy density. (*Lower*) Average energy breakdown between van der Waals (vdW) and electrostatic (ELEC) contributions. The average over the full trajectory was obtained by analyzing all individual DMPC/GA pairs. The large peak centered at zero corresponds to distant lipids that are weakly interacting with the channel.

data, the observed structural flexibility is supported by recent measurements indicating that χ_1 of Val[1] is ≈75% trans (25). In qualitative agreement with this experimental result, the simulations showed populations of 85% trans and 15% gauche for Val[1] of one monomer.

In contrast to the aliphatic side chains, the tryptophan side chains are stabilized by the membrane environment, fluctuating around well-defined conformations with the indole NH pointing toward the bulk solution. In the absence of the membrane, the tryptophans would have substantial conformational freedom: a systematic search shows that χ_1 can vary from 180 to 300 degrees, and χ_2 from 60 to 300 degrees. Test simulations of the channel in vacuum showed that large tryptophan fluctuations ultimately lead to the destabilization and unfolding of the β-helical dimer near the C terminus. The averages of the χ_1 and χ_2 dihedral angles from the molecular dynamics simulation are similar to those Arseniev *et al.* (24) determined from two-dimensional NMR of the dimer in SDS micelles (Table 1). This indicates that the SDS structure is consistent with the solid-state NMR data in oriented membranes.

Lipid–Protein Interactions. The agreement of the molecular dynamics average with experimental data provides confidence in the present model, suggesting that it can be used to gain insight into the details of lipid–protein interactions at the molecular level. The energy density shown in Fig. 4 is the distribution function of individual interaction energies between a DMPC molecule and GA, averaged over all possible pairs and over all the configurations along the trajectory. The total interaction energy between any single DMPC and GA extends over a very large range of energies from 0 to −50 kcal/mol. Decomposition of the interactions reveals that the average energy balance varies from exclusively vdW to nearly equal contributions of vdW and electrostatic terms. The most energetically favorable configurations involve both alkane-chain and headgroup interactions and were short-lived. This is in contrast with boundary lipid models (26), though the relatively high concentration of channel in the simulation system prevents further comparison.

The distribution functions of side chain–lipid interaction energies and their decomposition are shown in Fig. 5. As indicated by the significant contribution from the electrostatic interaction, the tryptophan side chains are capable of forming hydrogen bonds with the ester carbonyl groups of the lipids and the water, whereas the leucine side chains are not. The existence of these hydrogen bonds for the tryptophans are consistent with ^{2}H exchange and IR studies (27, 28). For both leucine and tryptophan side chains, the alkane chains are energetically the strongest interacting component. Next in importance is the glycerol region and water, both of which can form hydrogen bonds with the tryptophans. The choline headgroup is least important. These results show the difference between two residues located at the interface: the hydrophobic leucine and the amphipathic tryptophan.

The influence of lipid–protein interactions is also reflected in the average conformation of the lipid alkane chains. The chains were partially ordered by the GA in the simulation. This resulted in a decrease in the percent gauche from 25% to 23% within the hydrocarbon chains and by an increase in the average order parameter from −0.18 to −0.22, averaged over the whole trajectory and over both alkane chains. This is consistent with ^{2}H quadrupolar measurements and Fourier-transform IR studies, which have suggested that there should be a partial ordering of the alkane chains with this concentration of GA (29, 30). The relation of the bilayer thickness to the order of the hydrocarbon chains is a central assumption in the "mattress" model of lipid–protein interactions (31). A slight increase in the thickness of the bilayer,

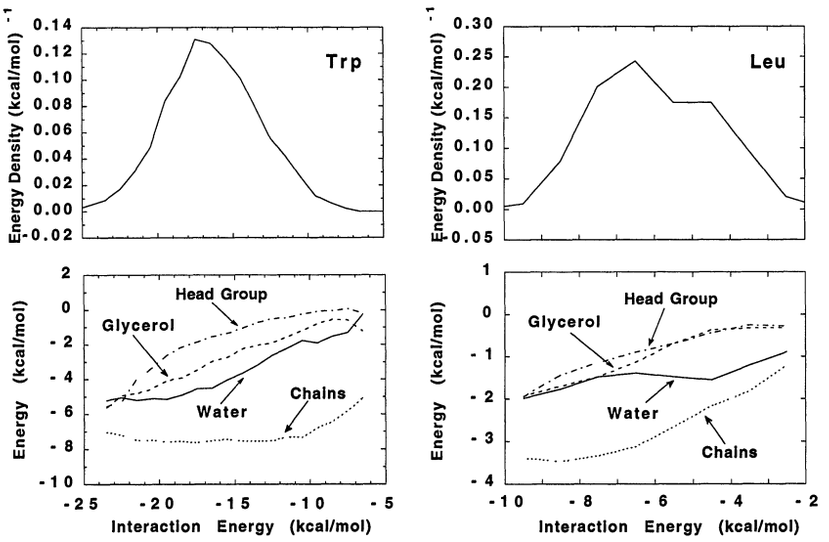

FIG. 5. Average distribution of interaction energies between the tryptophan (residues 9, 11, 13, and 15) and leucine (residues 10, 12, and 14) side chains and the fully hydrated membrane system. (*Upper*) Total average energy density. (*Lower*) Average energy contribution from water, alkane chains, glycerol region, and choline headgroup. The average was performed by analyzing the total interaction energy between the individual side chain and the hydrated membrane for all configurations.

from 34 to 36 Å, is observed, in accord with the partial ordering of the alkane chains. For the headgroups, the ^{31}P chemical shift anisotropy averaged −29 ppm over the simulation, which compares favorably with experimental values of −33 and −31 ppm for this concentration of DMPC/GA (32). This indicates a non-negligible influence of GA on the headgroup orientation, since the ^{31}P chemical shift anisotropy is −48 ppm for pure bilayers (33).

DISCUSSION

Molecular dynamics provides an effective method for exploring the microscopic details of membrane–protein interactions. The enormous body of experimental data concerning the small gramicidin channel allows a critical examination of the computed trajectory. The excellent agreement between calculations and experiment suggest that the present microscopic model may be used to gain insight into the details of lipid–protein interactions. Analysis of the trajectory reveals the complexity of the membrane/solution interface and the range of possible interactions. In particular, the tryptophan residues are shown to play an important role in mediating interactions between the lipid glycerol region and the protein, possibly leading to increased stability of the protein in the bilayer. Most of the nonpolar residues with aliphatic side chains are observed to undergo isomerization transitions between multiple conformations. In contrast, the tryptophan side chains fluctuate around a well-defined conformation stabilized by the membrane. Their hydrophobic moiety is buried in the hydrocarbon region and their indole NH group is pointing toward the bulk solution, where it can make hydrogen bonds with the lipid glycerol backbone or with interfacial waters. The nature of the lipid–protein interactions in the hydrophilic/hydrophobic interfacial region is thus considerably more complex than may have been expected from simpler macroscopic models. This suggests that thermodynamic partition studies using water/glycerol/phosphocholine mixtures may be useful for understanding the contribution of residues located inside the interfacial region to the stability of membrane proteins.

We are grateful to B. J. Hardy, R. M. Venable, and R. W. Pastor for providing the library of 2000 preequilibrated dipalmitoyl phosphatidylcholine molecules and to A. D. MacKerell and M. Karplus for providing the all-hydrogen CHARM 22 force field for proteins and phospholipids prior to publication. This research was supported by the Medical Research Council of Canada and by the Membrane Transport Research Group. B.R. is a Fonds de la Recherche en Santé du Québec Research Fellow.

1. Eisenberg, D., Weiss, R. M. & Terwilliger, T. C. (1982) *Nature (London)* **299**, 371–374.
2. Engelman, D. M., Steitz, T. A. & Goldman, A. (1986) *Annu. Rev. Biophys. Biophys. Chem.* **15**, 321–353.
3. Jacobs, R. E. & White, S. H. (1989) *Biochemistry* **28**, 3421–3437.
4. Brooks, C. B., III, Karplus, M. & Montgomery Pettitt, B. (1988) *Proteins: A Theoretical Perspective of Dynamics, Structure, and Thermodynamics* (Wiley, New York).
5. Heller, H., Schaefer, M. & Schulten, K. (1993) *J. Phys. Chem.* **97**, 8343–8360.
6. Ketchem, R. R., Hu, W. & Cross, T. A. (1993) *Science* **261**, 1457–1460.
7. Smith, R., Thomas, D. E., Separovic, F., Atkins, A. R. & Cornell, B. A. (1989) *Biophys. J.* **56**, 307–314.
8. Prosser, R. S., Davis, J. H., Dahlquist, F. W. & Lindorfer, M. A. (1991) *Biochemistry* **30**, 4687–4696.
9. Roux, B. & Karplus, M. (1994) in *Annu. Rev. Biophys. Biomol. Struct.* **23**, 731–761.
10. Andersen, O. S. & Koeppe, R. E., II (1992) *Physiol. Rev.* **72**, S89–S158.
11. Deisenhofer, J. & Michel, H. (1989) *Science* **245**, 1463–1473.
12. Swairjo, M. A. & Seaton, B. A. (1994) *Annu. Rev. Biophys. Biomol. Struct.* **23**, 193–213.
13. Cowan, S. W., Schirmer, T., Rummel, G., Steiert, M., Ghosh, R., Pauptit, R. A., Jansonius, J. N. & Rosenbusch, J. P. (1992) *Nature (London)* **358**, 727–733.
14. Weiss, M. S. & Schulz, G. E. (1992) *J. Mol. Biol.* **227**, 493–509.
15. Becker, M. D., Greathouse, D. V., Koeppe, R. E., II, & Andersen, O. S. (1991) *Biochemistry* **30**, 8830–8839.
16. Pascher, I., Lundmark, M., Nyholm, P. G. & Sundell, S. (1992) *Biochim. Biophys. Acta* **1113**, 339–373.
17. Bechinger, B. & Seelig, J. (1991) *Chem. Phys. Lipids* **58**, 1–5.
18. Venable, R. M., Zhang, Y., Hardy, B. J. & Pastor, R. W. (1993) *Science* **262**, 223–226.
19. Woolf, T. B. & Roux, B. (1994) *J. Am. Chem. Soc.* **116**, 5916–5926.
20. Engelman, D. M. & Lewis, B. A. (1983) *J. Mol. Biol.* **166**, 211–217.
21. Pastor, R. W., Venable, R. M. & Karplus, M. (1991) *Proc. Natl. Acad. Sci. USA* **88**, 892–896.
22. Zaccai, G., Buldt, G., Seelig, A. & Seelig, J. (1979) *J. Mol. Biol.* **134**, 693–706.
23. Damodaran, K. V., Merz, K. M., Jr., & Gaber, B. P. (1992) *Biochemistry* **31**, 7656–7664.
24. Arseniev, A. S., Barsukov, I. L., Bystrov, V. F., Lomize, A. L. & Ovchinnikov, Y. A. (1985) *FEBS Lett.* **186**, 168–174.
25. Lee, K. C. & Cross, T. A. (1994) *Biophys. J.* **66**, 1380–1387.
26. Owicki, J. C., Springgate, M. W. & McConnell, H. M. (1978) *Proc. Natl. Acad. Sci. USA* **75**, 1616–1619.
27. Takeuchi, H., Nemoto, Y. & Harada, I. (1990) *Biochemistry* **29**, 1572–1579.
28. Bouchard, M. & Auger, M. (1993) *Biophys. J.* **65**, 2484–2492.
29. Davies, M. A., Brauner, J. W., Schuster, H. F. & Mendelsohn, R. (1990) *Biochem. Biophys. Res. Commun.* **168**, 85–90.
30. Rice, D. & Oldfield, E. (1979) *Biochemistry* **18**, 3272–3279.
31. Mouritsen, O. G. & Bloom, M. (1984) *Biophys. J.* **46**, 141–153.
32. Moll, F., III, & Cross, T. A. (1990) *Biophys. J.* **57**, 351–362.
33. Seelig, J. (1978) *Biochim. Biophys. Acta* **515**, 105–140.